Measurement of Higgs boson mass and width with the ATLAS detector

Higgs 2023, Beijing

Zihang Jia[1,2] **on behalf of the ATLAS collaboration**

[1] *Institute of High Energy Physics, Chinese Academy of Science*

[2] *Nanjing University*

Introduction

- The Higgs boson plays a unique role in the standard model (SM) giving masses to other particles via electroweak spontaneous symmetry breaking.
- Since its discovery in 2012, efforts have been made to determine its properties.
- This talk will focus on the latest ATLAS measurements of the Higgs boson **mass** m_H and **width** Γ_H .

Standard Model of Elementary Particles

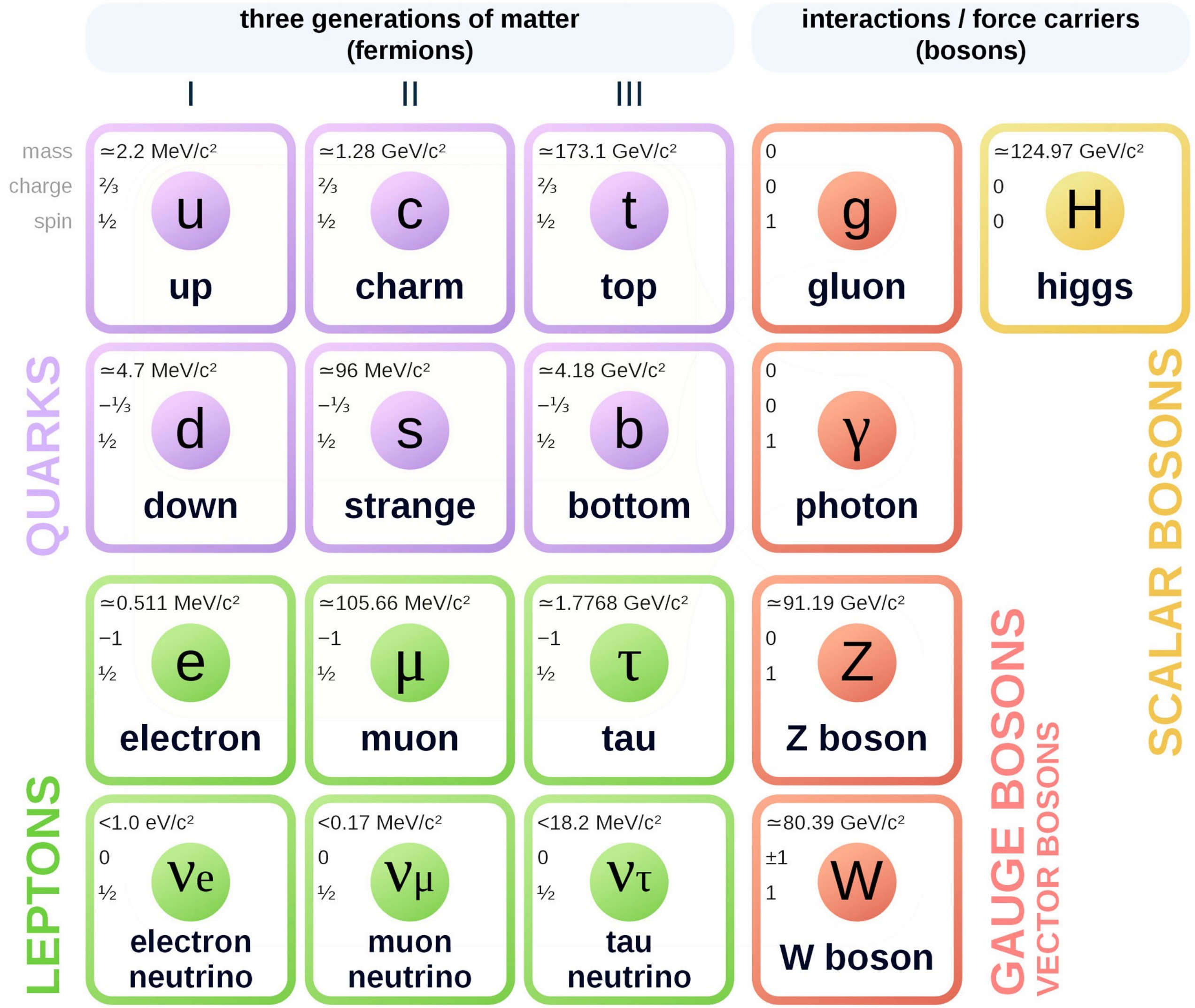

Higgs boson mass

Higgs boson mass measurement

The **Higgs mass** m_H is a free parameter of the standard model that **must be determined experimentally**

Measurements are made in the $\boldsymbol{H \to ZZ^* \to 4l}$ and $\boldsymbol{H \to \gamma\gamma}$ channels due to their **excellent mass resolution**

➔ Previous ATLAS results with **partial Run 2 + Run 1** data gave a mass of **m_H = 124.97 ± 0.24 GeV**

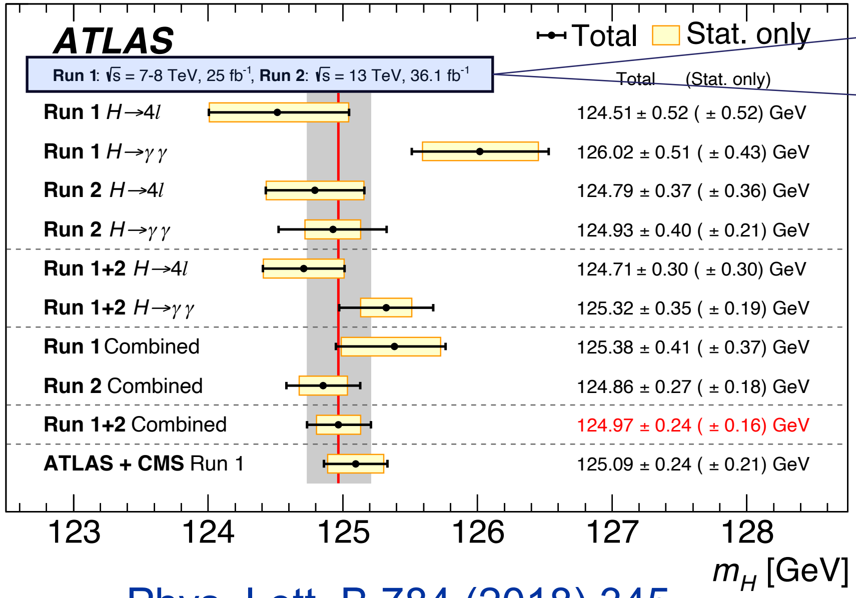

Phys. Lett. B 784 (2018) 345

Now: 25 + **140 fb^{-1}**

Results are now updated with full Run 2 datatset with luminosity increased by a factor of ~ 3

$H \to ZZ^* \to 4l$ channel

The signal is a **narrow resonant peak above a continuum background in the m_{4l} distribution**

Main background from non-resonant ZZ* production (~89% of the total background yield)

Select events containing **at least four isolated leptons** emerging from a common vertex

Four final states considered: $4\mu, 4e, 2\mu 2e, 2e 2\mu$

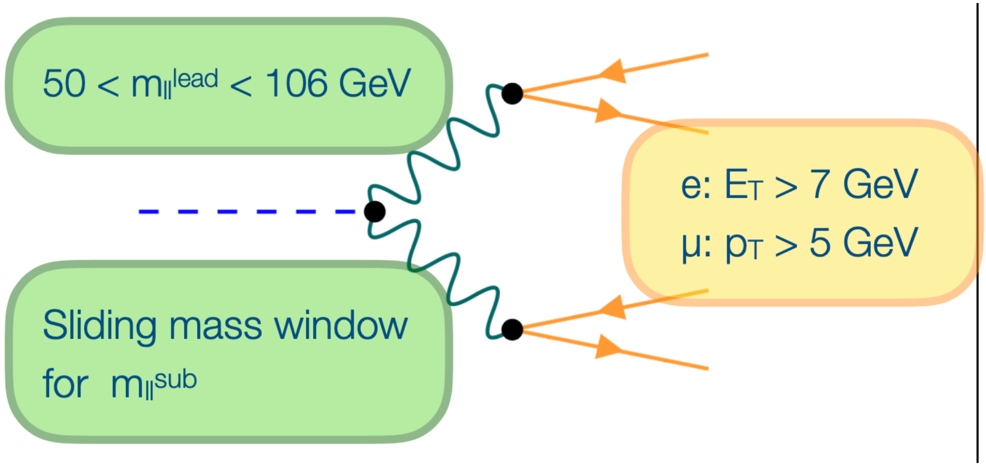

[Phys. Lett. B 843 (2023) 137880]

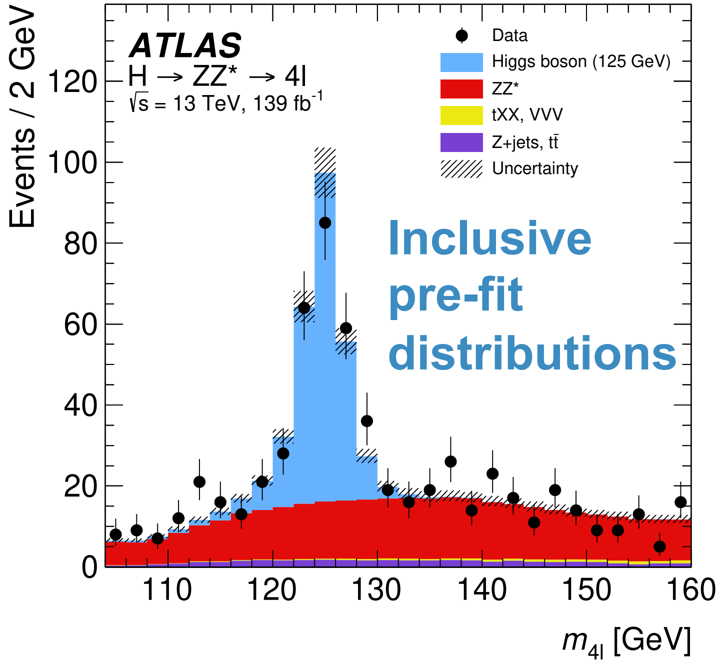

$H \rightarrow ZZ^* \rightarrow 4l$ channel

Signal-background discriminant D_{NN}: **neural network** (NN) classifier against the ZZ* background

Per-event resolution σ_i: **quantile regression neural network** (QRNN) to predict event-level m_{4l} resolution

➔ Output is the predicted quantile of the difference between the reconstructed m_{4l} and the true m_{4l}

Phys. Lett. B 843 (2023) 137880

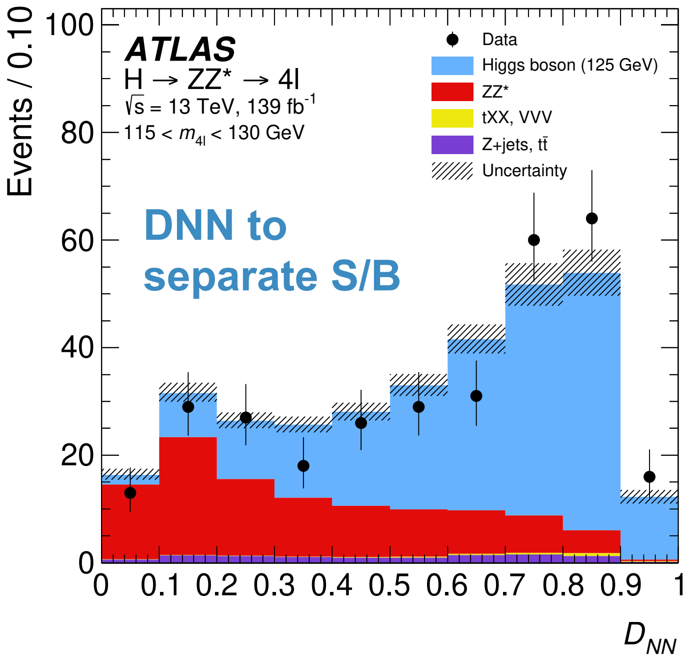

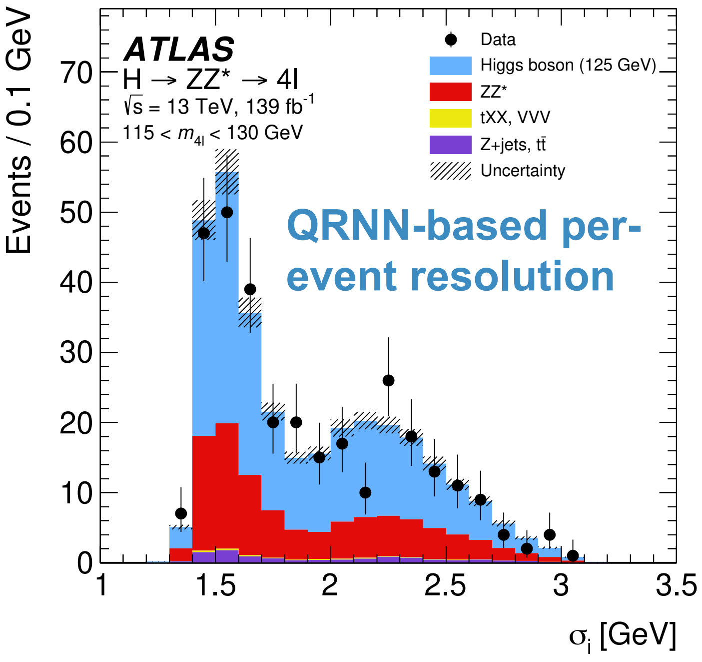

$H \to ZZ^* \to 4l$ channel

Higgs mass extraction: maximum-likelihood fit in the four decay channels across three variables: m_H, D_{NN}, σ_i

- **Signal model:** Double-sided Crystal-Ball, capturing dependencies on m_H, D_{NN} and σ_i
- **Background model:** 2D probability density function (m_H, D_{NN}) smoothed using **kernel estimation**

Phys. Lett. B 843 (2023) 137880

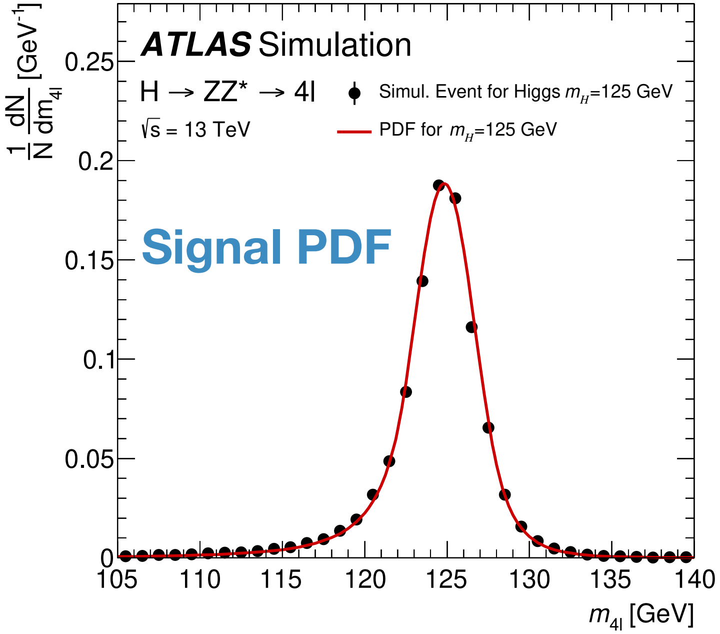

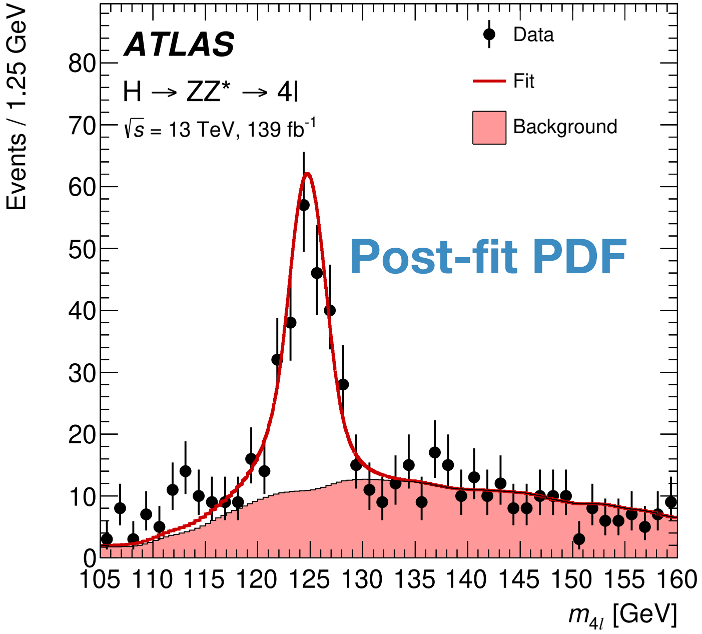

$H \rightarrow ZZ^* \rightarrow 4l$ channel

Run 2: m_H = 124.99 ± 0.18 (stat.) ± 0.04 (syst.) GeV

Phys. Lett. B 843 (2023) 137880

Systematic Uncertainty	Contribution [MeV]
Muon momentum scale	± 28
Electron energy scale	± 19
Signal-process theory	± 14

Still statistical uncertainty dominant

Phys. Lett. B 843 (2023) 137880

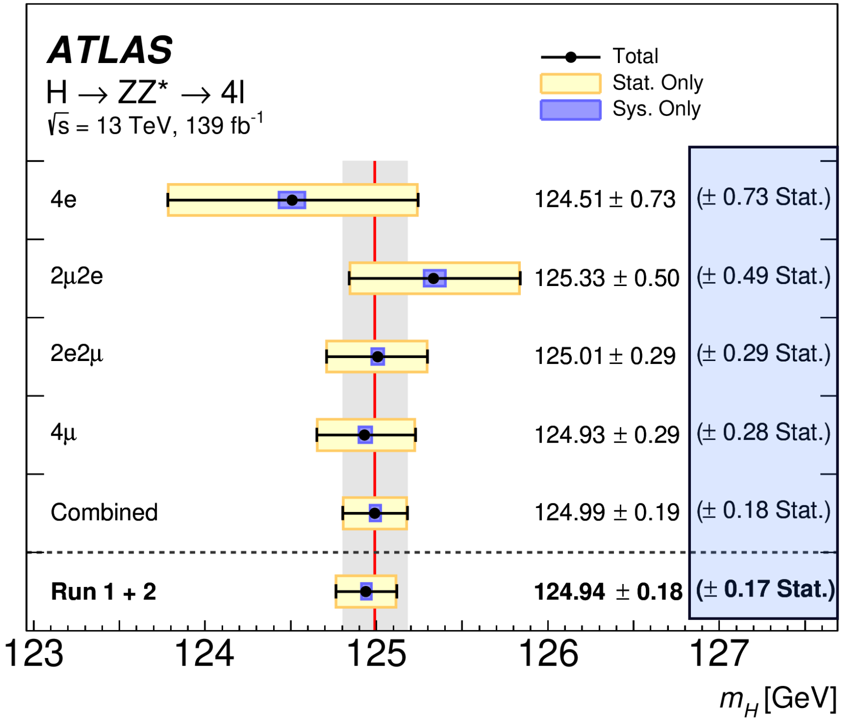

Sources of improvements

- **Neural-network-based** signal-background discriminant D_{NN} (precision improved by 2%)
- **Event-by-event m_{4l} resolution** σ_i in the analytic model (uncertainty reduced by 1%)
- New high-precision **muon momentum calibration**

The muon scale uncertainty was reduced **by a factor of 4** compared to previous results.

$H \rightarrow \gamma\gamma$ channel

The signal is **a narrow peak over a large non-resonant background in the $m_{\gamma\gamma}$ distribution**

Main background from non-resonant $pp \rightarrow \gamma\gamma$**+partons** production

Select events with **two good quality photons** with $p_T^{\gamma}/m_{\gamma\gamma}$ > 0.35 (0.25)

Phys. Lett. B 847 (2023) 138315

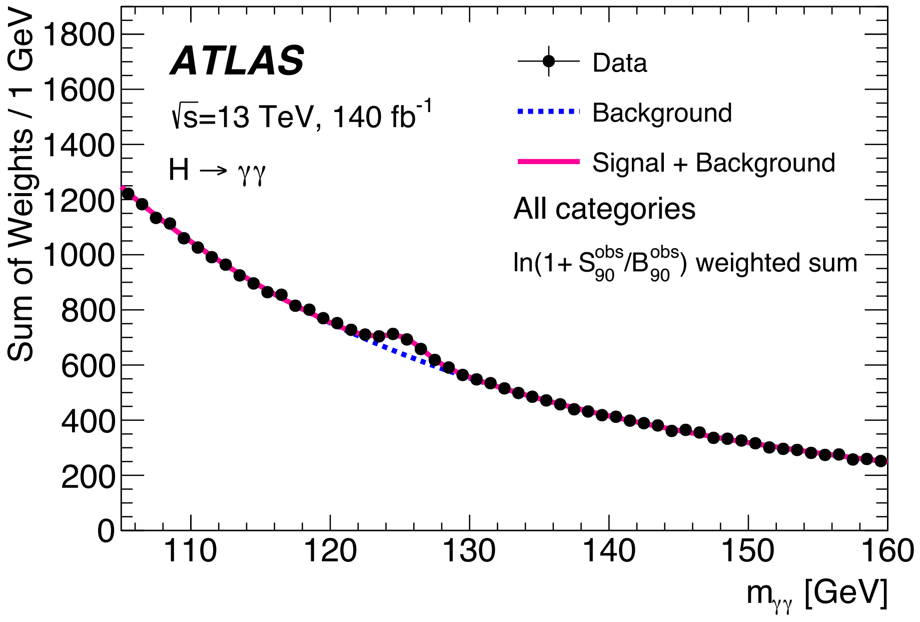

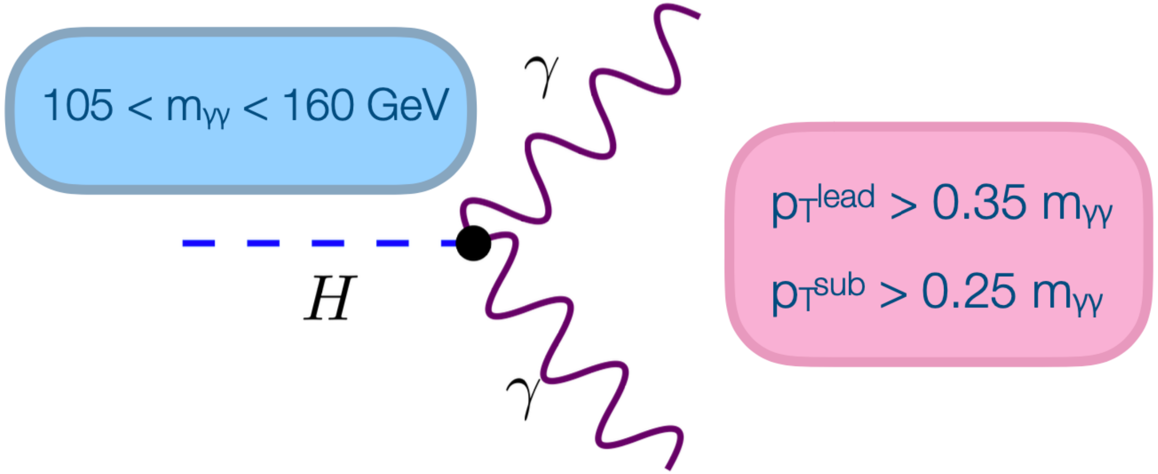

$H \to \gamma\gamma$ channel

To increase the sensitivity of the measurement

14 mutually exclusive categories based on

- The number of **converted photons**
- **Pseudorapidity** of photon pairs
- Diphoton **transverse momentum**

Phys. Lett. B 847 (2023) 138315

	Central-barrel	Outer-barrel	Endcap
C-type (>0 γ_{conv})	high p_{Tt}	high p_{Tt}	
	medium p_{Tt}	medium p_{Tt}	
	low p_{Tt}	low p_{Tt}	
U-type (0 γ_{conv})	high p_{Tt}	high p_{Tt}	
	medium p_{Tt}	medium p_{Tt}	
	low p_{Tt}	low p_{Tt}	

Phys. Lett. B 847 (2023) 138315

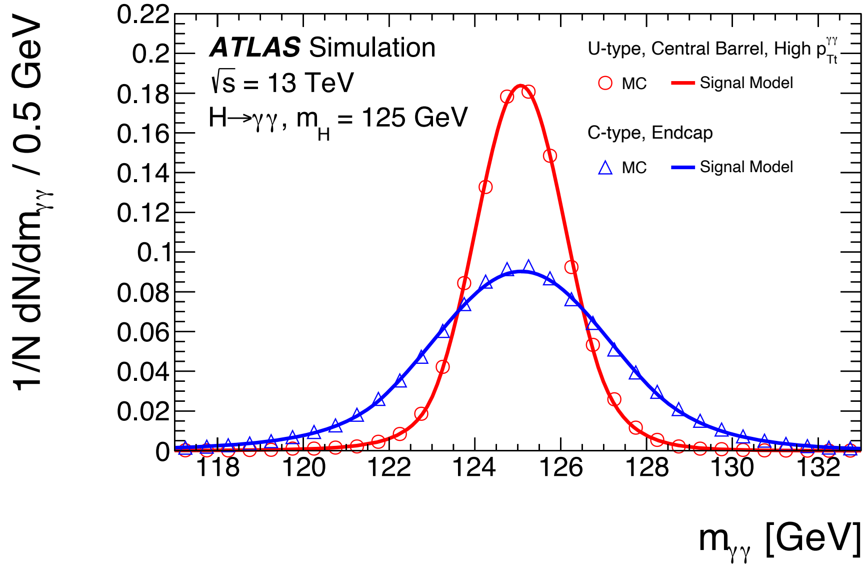

- **Signal model:** Double-sided Crystal-Ball function with peak position and resolution parameterized as functions of m_H
- **Background model:** chosen among exponential, power-law or an exponentiated 2nd-order polynomial functions empirically for each category based on goodness-of-fit

m_H is evaluated by signal+background maximum-likelihood fit

$H \to \gamma\gamma$ channel

Run 2: m_H = 125.17 ± 0.11 (stat.) ± 0.09 (syst.) GeV

Source	Impact [MeV]
Photon energy scale	83
$Z \to e^+e^-$ calibration	59
E_T-dependent electron energy scale	44
$e^\pm \to \gamma$ extrapolation	30
Conversion modelling	24
Signal–background interference	26
Resolution	15
Background model	14
Selection of the diphoton production vertex	5
Signal model	1
Total	90

Phys. Lett. B 847 (2023) 138315

Sources of improvements:

- **Improved estimation of the photon energy scale with reduced uncertainties**
- New **photon reconstruction algorithm** with better energy resolution
- Optimised **event classification strategy**

Now statistical uncertainty dominated again, unlike the intermediate Run 2 publication

Phys. Lett. B 847 (2023) 138315

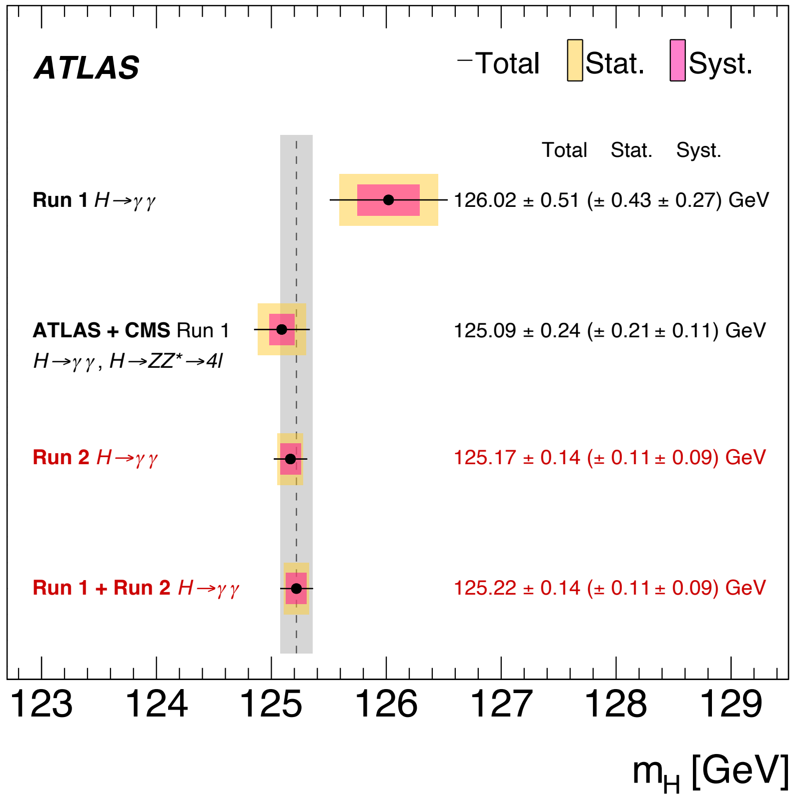

The photon energy scale systematics improved by **a factor of ~4** (ATLAS Run 2 Calibration paper)

ATLAS EXPERIMENT

Combined measurement

Combination of the ATLAS Run 1 + Run 2 m_H measurement in $H \to ZZ^* \to 4l$ and $H \to \gamma\gamma$ final states

m_H = 125.11 ± 0.09 (stat.) ± 0.06 (syst.) = 125.11 ± 0.11 GeV

Partial Run 2

Phys. Lett. B 784 (2018) 345

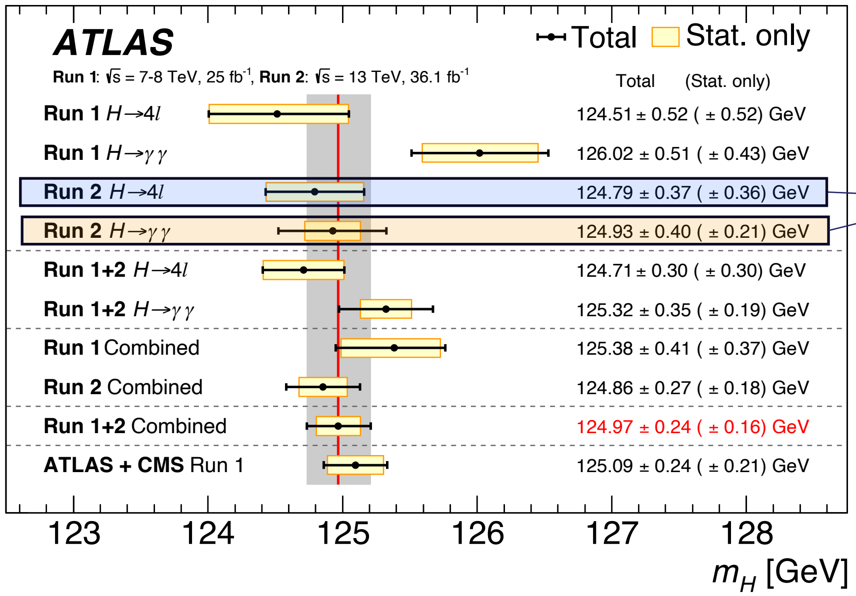

arXiv:2308.04775

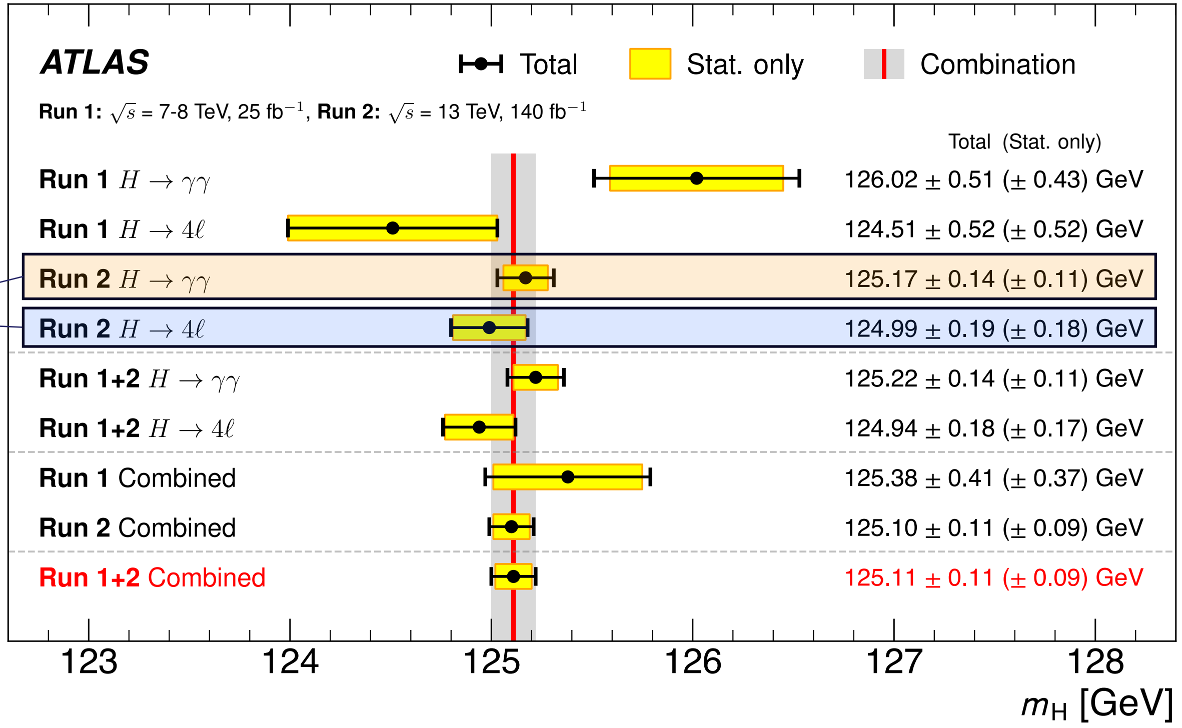

➔ Current **most precise m_H measurement** reaching a **precision of 0.09%**

Higgs boson width

Higgs boson width measurement

The **Higgs width** Γ_H contains information about the Higgs interactions **with all other fundamental particles**

Direct measurement: limited by detector resolution (predicted 4.1 MeV compared with 1-2 GeV)

Indirect measurement: rely on both on-shell and off-shell Higgs boson production

$$\Gamma_H \propto \frac{\mu_{off-shell}}{\mu_{on-shell}}$$

Assuming that the on-shell and off-shell Higgs production follow SM prediction

On-shell region: $s \sim m_H^2$
Close to Higgs resonant peak
$$\sigma_{on-shell} \propto \frac{g_{prod}^2 \times g_{decay}^2}{\Gamma_H}$$

Off-shell region: $s \gg m_H^2$
Far from Higgs resonant peak
$$\sigma_{off-shell} \propto g_{prod}^2 \times g_{decay}^2$$

JHEP 08 (2012) 116

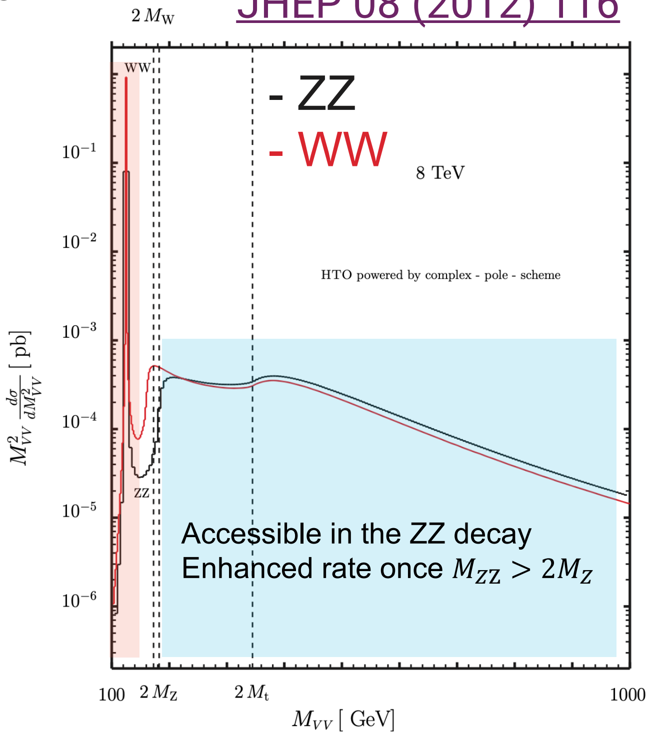

$H^* \rightarrow ZZ$ channel

Negative interference between the **off-shell Higgs boson process** and the **continuum background**

The signal is a **deficit** in **gluon fusion (ggF)** or **electroweak (EW VBF+VH)** production

- **Three signal regions (SRs) targeting both production modes:**

  EW SR: ≥ 2 jets with p_T > 30 GeV, well-separated leading jets ($|\Delta\eta_{jj}| > 4$)

  Mixed SR: Failing EW SR but with exactly 1 forward jet ($|\Delta\eta_{jj}| > 2.2$)

  ggF SR: All other events passing event selection

Distributions of discriminating variables are fitted simultaneously in all SRs

Control Regions also included in the fit to constrain the background normalisation

Phys. Lett. B 846 (2023) 138223

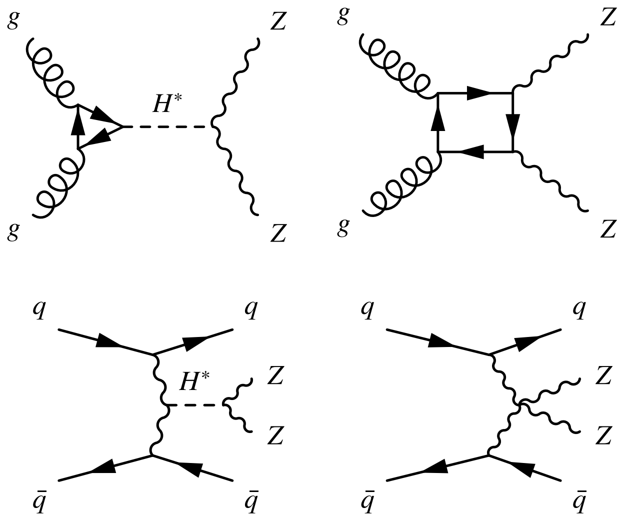

$H^* \to ZZ$ channel

➢ **Two final states are separately analysed and then combined to obtain the final results**

$ZZ \to 4l$

Fully reconstructible final state

Clean signature, main background qqZZ

Observable: Neural network (NN) output

Phys. Lett. B 846 (2023) 138223

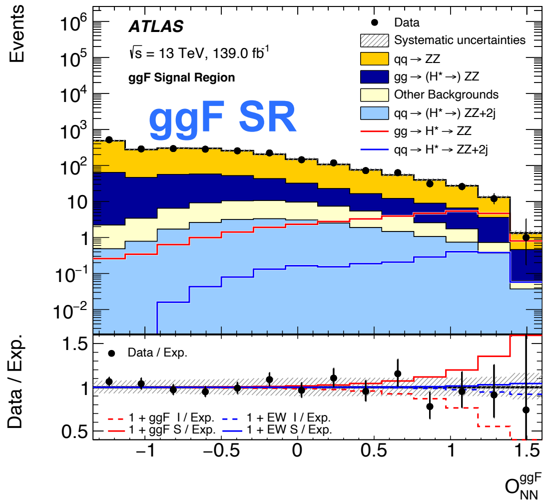

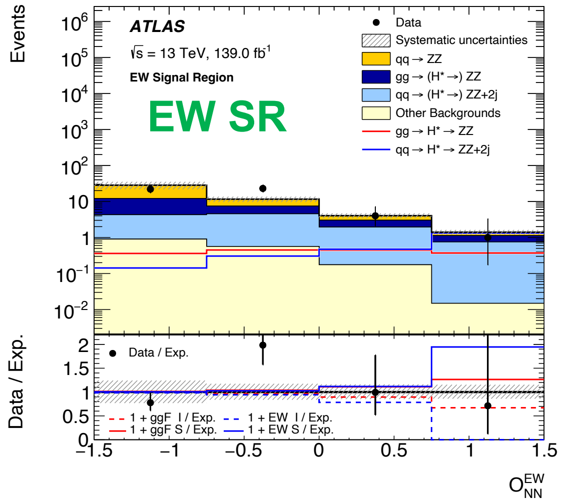

$ZZ \to 2l2\nu$

Six times higher branching ratio

Larger background contamination

Observable: Transverse ZZ mass m_T^{ZZ}

Phys. Lett. B 846 (2023) 138223

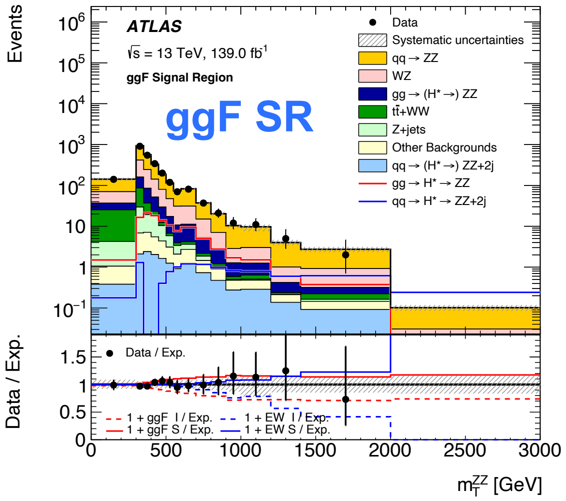

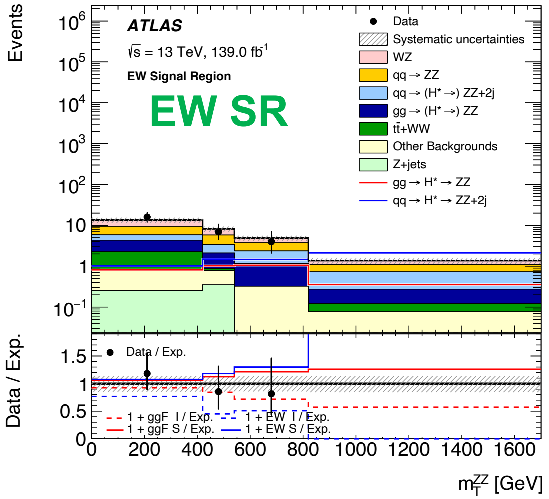

ATLAS EXPERIMENT

$H^* \rightarrow ZZ$ channel

Combined with on-shell $4l$ channel measurement (Eur. Phys. J. C 80 (2020) 942)

- **Direct measurement of off-shell H production**

$$\mu_{off-shell} = 1.1^{+0.7}_{-0.6}$$

Background-only hypothesis rejected at 3.3 σ

Evidence

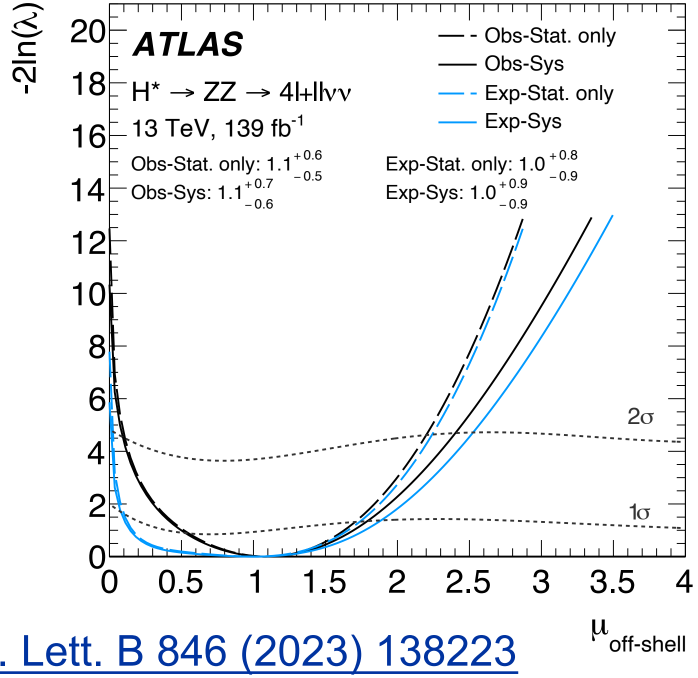

Phys. Lett. B 846 (2023) 138223

- **Higgs width determination**

$$\Gamma_H = 4.5^{+3.3}_{-2.5}\ \text{MeV}$$

Compatible with the SM prediction at 4.1 MeV

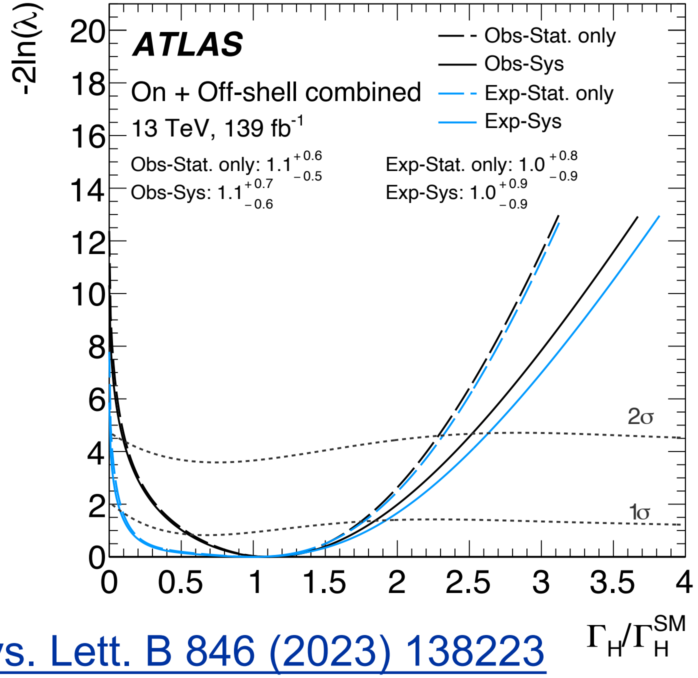

Phys. Lett. B 846 (2023) 138223

Conclusion

m_H = 125.11 ± 0.09 (stat.) ± 0.06 (syst.) = 125.11 ± 0.11 GeV

Run 1 + Run 2 Higgs mass measurement by combining $H \to ZZ^* \to 4l$ and $H \to \gamma\gamma$ final states

Current **most precise m_H measurement** with an uncertainty of 0.09%

Benefit from **excellent Run 2 calibration** of e, γ, μ

Statistical uncertainty remains dominant (as in Run 1)

Phys. Lett. B 843 (2023) 137880
Phys. Lett. B 847 (2023) 138315
arXiv:2308.04775 (accepted by PRL)

Run 2 indirect Higgs width measurement from off-shell Higgs production in ZZ channel

First evidence of off-shell Higgs production with a significance of 3.3σ

Off-shell yields are still **limited by statistics**

Room for improvements in the **systematic uncertainties** (e.g. theoretical modeling)

$\Gamma_H = 4.5^{+3.3}_{-2.5}$ MeV

Phys. Lett. B 846 (2023) 138223

Stay tuned for more Run 2 measurements and for Run 3!

Thank you for your attention!

Back-up

References

ATLAS $H \to ZZ^* \to 4l$ m_H Run 2 measurement: Phys. Lett. B 843 (2023) 137880, Aux figures HIGG-2020-07

ATLAS $H \to \gamma\gamma$ m_H Run 1 measurement: Phys. Rev. D 98 (2018) 052005, Aux figures HIGG-2016-21

ATLAS $H \to \gamma\gamma$ m_H Run 2 measurement: Phys. Lett. B 847 (2023) 138315, arXiv:2308.07216, Aux figures HIGG-2019-16

ATLAS $H \to ZZ^* \to 4l$ *and* $H \to \gamma\gamma$ m_H partial Run 2 measurement: Phys. Lett. B 784 (2018) 345, Aux figures HIGG-2016-33

ATLAS $H \to ZZ^* \to 4l$ and $H \to \gamma\gamma$ m_H Run 1 + Run 2 measurement: arXiv:2308.04775, Aux figures HIGG-2022-20

ATLAS+CMS m_H Run 1 measurement: PhysRevLett.114.191803

ATLAS Run 2 electron and photon energy calibration: arXiv:2309.05471

ATLAS $H^* \to ZZ$ Γ_H Run 1 measurement: Phys. Lett. B 786 (2018) 223, Aux figures HIGG-2017-06

ATLAS $H^* \to ZZ$ Γ_H Run 2 measurement: Phys. Lett. B 846 (2023) 138223, arXiv:2304.01532, Aux figures HIGG-2018-32

CMS m_H and Γ_H Run 2 measurement: HIG-21-019

CMS Γ_H partial Run 2 measurement: Nature Phys. 18 (2022) 1329

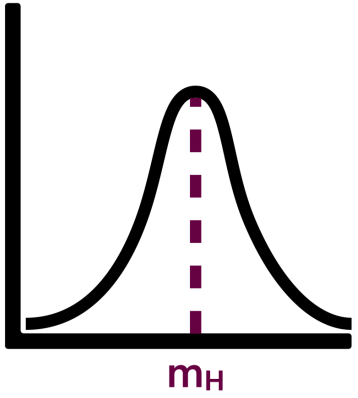

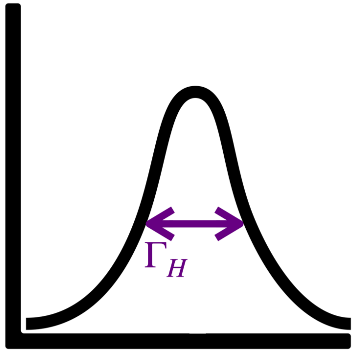

Higgs boson mass

The **Higgs mass** m_H is a free parameter of the standard model that **must be determined experimentally**

- It governs the coupling strengths of the Higgs boson with the other SM particles
  - It is also the value assumed by the experimental collaborations when estimating the acceptances, efficiencies and signal models used in their analyses and to report their measured rates
- It is one of the inputs in global fits to the measurements of electroweak observables
- It determines the shape of the Higgs potential and thus the stability of the electroweak vacuum

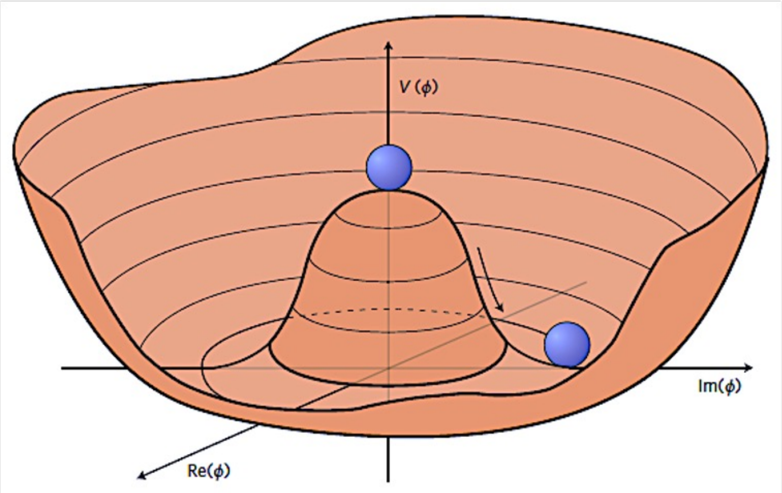

$$\mathscr{L} \subset V(\phi) = V_0 + \frac{1}{2}m_H^2 H^2 + \lambda v H^3 + \frac{1}{4}\lambda H^4$$

ATLAS m_H measurement in $H \to ZZ^* \to 4l$ channel

FSR recovery and the Z mass constraint

FSR recovery (resolution improved by 1%): From simulation, it is estimated that ~ 3% of signal events are affected by FSR, recovery algorithm is used to target and recover these FSR particles.

Z mass constraint (resolution improved by 17%): The leading lepton pair is predominantly produced from the decay of an **on-shell** Z-boson. ZMC allows for an improvement in the 4-lepton mass resolution by **constraining the $\mathbf{m_{12}}$ to the Z line shape** using the lepton momentum and its uncertainties.

ATLAS EXPERIMENT

ATLAS m_H measurement in $H \rightarrow ZZ^* \rightarrow 4l$ channel

Likelihood

- In general the model we want is: $\mathcal{L}(m_H|\boldsymbol{x}) = \mathcal{L}(m_H|m_{4\ell}, D, \sigma) = \prod_i P(m^i_{4\ell}, D^i, \sigma^i | m_H)$
- However, we do not have infinite MC statistics and computing so we must simplify

- For signal we can decompose as: $P_s(m_{4\ell}, D, \sigma|m_H) = P_s(m_{4\ell}|D, \sigma, m_H) \cdot P_s(D, \sigma|m_H) = P_s(m_{4\ell}|D, \sigma, m_H) \cdot P_s(D|\sigma, m_H) \cdot P_s(\sigma|m_H)$
- For the CONF, we fitted a DCB in 4 bins of D and in each channel, ignoring the last term

$$P_s(m_{4\ell}|D, \sigma, m_H) = \sum_{j \in D_{bins}} DCB(\mu = f^j_\mu(m_H), w = f^j_\sigma(\sigma), \alpha^j_{Lo}, n^j_{Lo}, \alpha^j_{Hi}, n^j_H|\sigma)$$

- This round, we want to make the signal continuous on D to simplify the implementation of systematics on the Discriminant side

- For background we can decompose as: $P_b = P_b(m_{4\ell}, D) \cdot P_b(\sigma)$
- Where in the last round we smoothed $P_b(m_{4\ell}, D) = \sum_{j \in D_{bins}} P_b(m_{4\ell})^j$
- Now aim to use $P(m_{4l}, D)$ to take into account the full dependance on discriminant - For binned setup, had to assign large sys to account variation of resolution vs D

ATLAS m_H measurement in $H \rightarrow ZZ^* \rightarrow 4l$ channel

The improvement of muon scale systematics

Partial Run 2

Phys. Lett. B 784 (2018) 345

Systematic effect	Uncertainty on $m_H^{ZZ^*}$ [MeV]
Muon momentum scale	40
Electron energy scale	26
Pile-up simulation	10
Simulation statistics	8

→

Run 2

Phys. Lett. B 843 (2023) 137880

Systematic Uncertainty	Contribution [MeV]
Muon momentum scale	± 28
Electron energy scale	± 19
Signal-process theory	± 14

ATLAS m_H measurement in $H \to \gamma\gamma$ channel

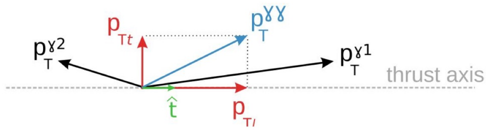

Categorization scheme

arXiv:2308.04775

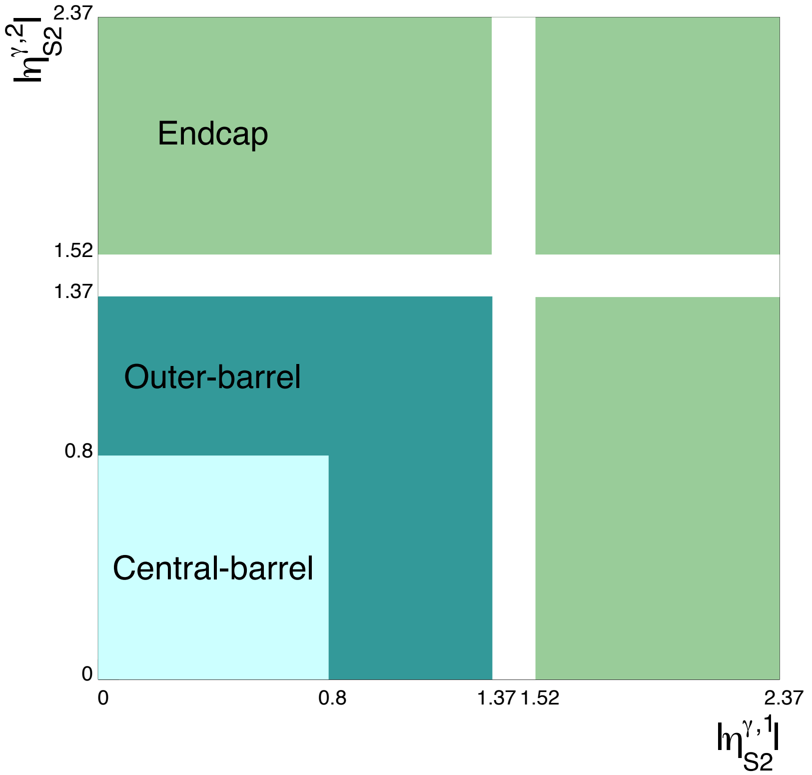

Gains on total m_H uncertainty based solely on the categorization

- -17% compared to inclusive measurement (1 category)
- -6% compared with 36 fb^{-1} analysis (31 categories)
- -3% compared to full Run2 STXS/coupling (101 categories)

ATLAS m_H measurement in $H \to \gamma\gamma$ channel

Signal modeling

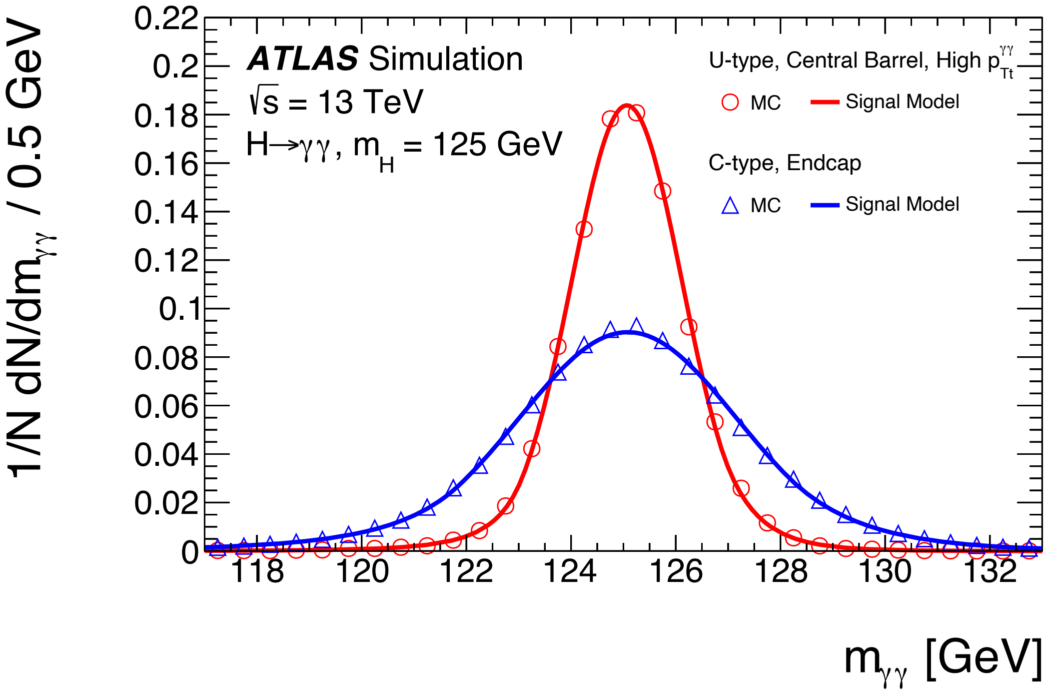

- Model m_{H} dependency of the DSCB parameters using signal MC samples at different m_{H}
  - Linear dependence for peak and resolution

$$\mu_{\mathrm{CB}}(m_{\mathrm{H}}) = m_{\mathrm{H}} + B_{\mu_{\mathrm{CB}}} + A_{\mu_{\mathrm{CB}}}(m_{\mathrm{H}} - 125\ \mathrm{GeV})$$
$$\sigma_{\mathrm{CB}}(m_{\mathrm{H}}) = B_{\sigma_{\mathrm{CB}}} + A_{\sigma_{\mathrm{CB}}}(m_{\mathrm{H}} - 125\ \mathrm{GeV})$$
$$\alpha_{\mathrm{Low}}(m_{\mathrm{H}}) = \alpha_{\mathrm{Low}} \qquad n_{\mathrm{Low}}(m_{\mathrm{H}}) = n_{\mathrm{Low}}|_{125\mathrm{GeV}}$$
$$\alpha_{\mathrm{High}}(m_{\mathrm{H}}) = \alpha_{\mathrm{High}} \qquad n_{\mathrm{High}}(m_{\mathrm{H}}) = n_{\mathrm{High}}|_{125\mathrm{GeV}}$$

- Signal yield variation with m_{H} parameterized with 2^{nd}-order polynominal, per category and prod-mode
- Signal model **extensively cross-checked** internally (global vs 125 GeV) and on the final workspace: **most extreme impact on m_{H} always $\leq$ 15 MeV**

ATLAS m_H measurement in $H \to \gamma\gamma$ channel

Background modeling

- χ^2 probability > 1% when fitted to the background template
- the fitted signal yield (the 'spurious signal') < 10% of the expected signal yield
- the fewest degrees of freedom

ATLAS m_H measurement in $H \rightarrow \gamma\gamma$ channel

The improvement of photon energy scale systematics

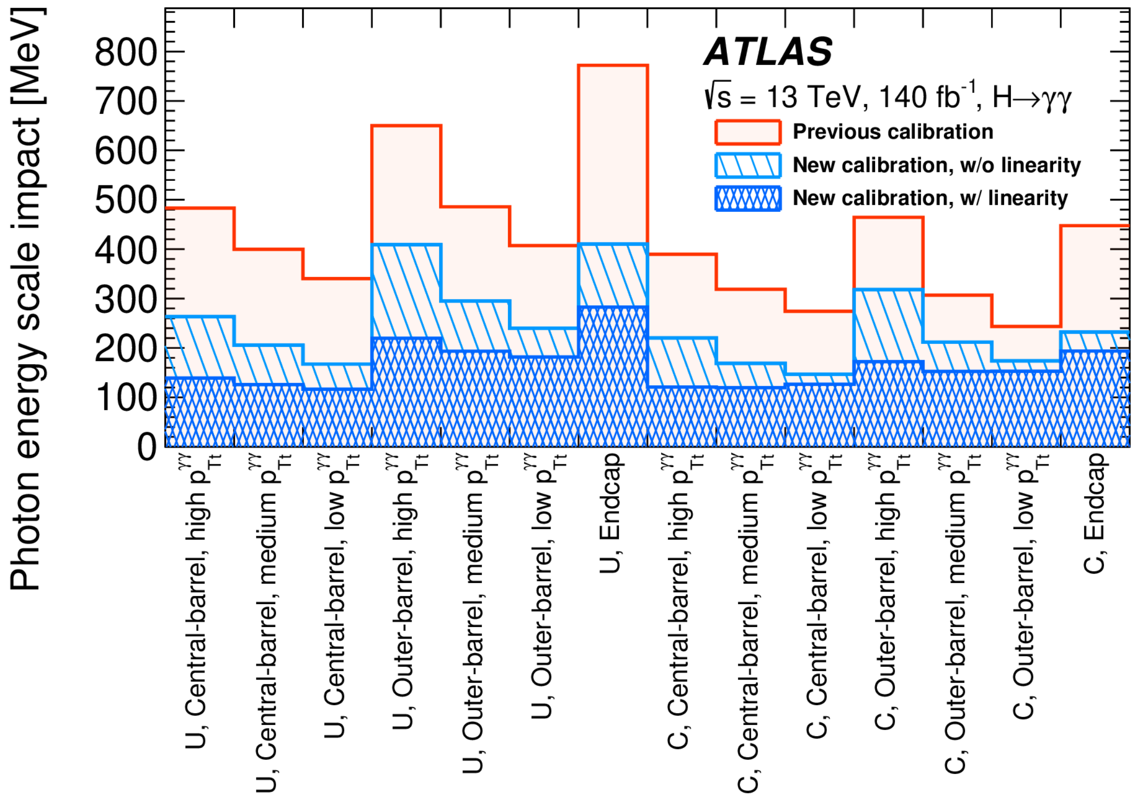

Only η**-dependent energy scale factors** were derived from 2015–2016 data

The possible E_T**-dependence** of the data-to-MC **electron** energy scale correction was accounted for

ATLAS EXPERIMENT

ATLAS m_H measurement in $H \to \gamma\gamma$ channel

Systematic uncertainties

Additional and secondary systematic uncertainties are included in the likelihood model

- **Signal and background modeling:** effect on m_{H} of a wrong functional form modelling
  - Evaluated injecting sig (bkg) MC sample over a bkg (sig) Asimov and computing the m_{H} shift
  - Effect uncorrelated among categories, impact of **5 (18) MeV for signal (background)**
- **Interference** between $pp \to \gamma\gamma$ and $pp \to H \to \gamma\gamma$ processes: causing a shift of the m_{H}
  - Evaluated by injecting interference MC sample over a S+B Asimov and computing the m_{H} shift
  - **Expected impact of** 24 MeV. **Decided not to correct for this**
- Photon energy resolution uncertainties
  - Evaluated as interquantile difference of $m_{\gamma\gamma}$ distribution per category, applied on width of DSCB
- Photon conversion reconstruction affecting category migrations
  - Estimated with data/MC comparison in $Z \to \ell\ell\gamma$ events, correlated to corresponding scale effect
- NN vertex selection effect on m_{H} (5 MeV)
  - Estimated with $Z \to ee$ data/MC comparision where e are treated as unconverted photons
- Lumi / BR $\gamma\gamma$/ QCD scale / PDF+α_S / Parton shower / Spurious signal
  - All included and with null impact on m_{H}

Partial Run 2

Phys. Lett. B 784 (2018) 345

Source	Systematic uncertainty on $m_H^{\gamma\gamma}$ [MeV]
EM calorimeter cell non-linearity	±180
EM calorimeter layer calibration	±170
Non-ID material	±120
ID material	±110
Lateral shower shape	±110
$Z \to ee$ calibration	±80
Conversion reconstruction	±50
Background model	±50
Selection of the diphoton production vertex	±40
Resolution	±20
Signal model	±20

Run 2

arXiv:2308.04775

Source	Systematic uncertainty in m_H [MeV]
Photon energy scale	±83
$Z \to e^+e^-$ calibration	±59
E_{T}-dependent electron energy scale	±44
$e^{\pm} \to \gamma$ extrapolation	±30
Conversion modelling	±24
Signal-background interference	±26
Resolution	±15
Background model	±14
Selection of the diphoton production vertex	±5
Signal model	±1
Total	±90

Impact extracted by fixing group of NPs and taking the difference with total uncertainty

ATLAS Run 2 Γ_H measurement

The observed and expected yields together with their uncertainties

$ZZ \to 4l$

Process	ggF SR	Mixed SR	EW SR
$gg \to (H^* \to)ZZ$	341 ± 117	42.5 ± 14.9	11.8 ± 4.3
$gg \to H^* \to ZZ$	32.6 ± 9.07	3.68 ± 1.03	1.58 ± 0.47
$gg \to ZZ$	345 ± 119	43.0 ± 15.2	11.9 ± 4.4
$qq \to (H^* \to)ZZ + 2j$	23.2 ± 1.0	2.03 ± 0.16	9.89 ± 0.96
$qq \to ZZ$	1878 ± 151	135 ± 23	22.0 ± 8.3
Other backgrounds	50.6 ± 2.5	1.79 ± 0.16	1.65 ± 0.16
Total expected (SM)	2293 ± 209	181 ± 29	45.3 ± 10.0
Observed	2327	178	50

$ZZ \to 2l2\nu$

Process	ggF SR	Mixed SR	EW SR
$gg \to (H^* \to)ZZ$	210 ± 53	19.7 ± 4.9	4.29 ± 1.10
$gg \to H^* \to ZZ$	111 ± 26	10.9 ± 2.5	3.26 ± 0.82
$gg \to ZZ$	251 ± 66	23.4 ± 6.2	5.31 ± 1.46
$qq \to (H^* \to)ZZ + 2j$	14.0 ± 3.0	1.63 ± 0.17	4.46 ± 0.50
$qq \to ZZ$	1422 ± 112	80.4 ± 11.9	7.74 ± 2.99
WZ	678 ± 54	51.9 ± 6.9	7.89 ± 2.50
Z+jets	62.3 ± 24.3	7.51 ± 6.94	0.62 ± 0.54
Non-resonant-$\ell\ell$	106 ± 39	9.17 ± 2.73	1.55 ± 0.42
Other backgrounds	22.6 ± 5.2	1.62 ± 0.25	1.40 ± 0.10
Total expected (SM)	2515 ± 165	172 ± 17	28.0 ± 4.1
Observed	2496	181	27

ATLAS Run 2 Γ_H measurement

Interference effects

- Yield dependence on $\mu_{off-shell}$ is not linear
- Asymptotic approximation does not hold
- Confidence intervals have to be derived using the **Neyman construction**
- 5-10% more conservative

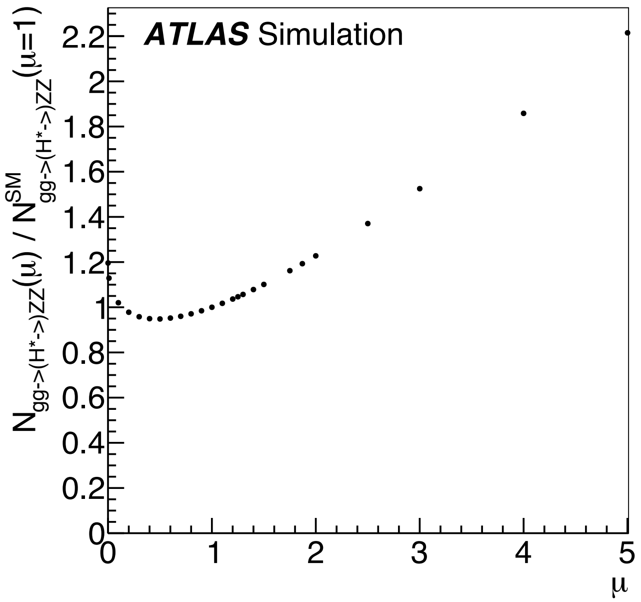

The expected curve is flatter than the observed due to the effect of **a downward fluctuation in the data** and **the parabolic shape of the yield versus μ curve**, which arises due to the $\sqrt{\mu}$ dependence of the interference

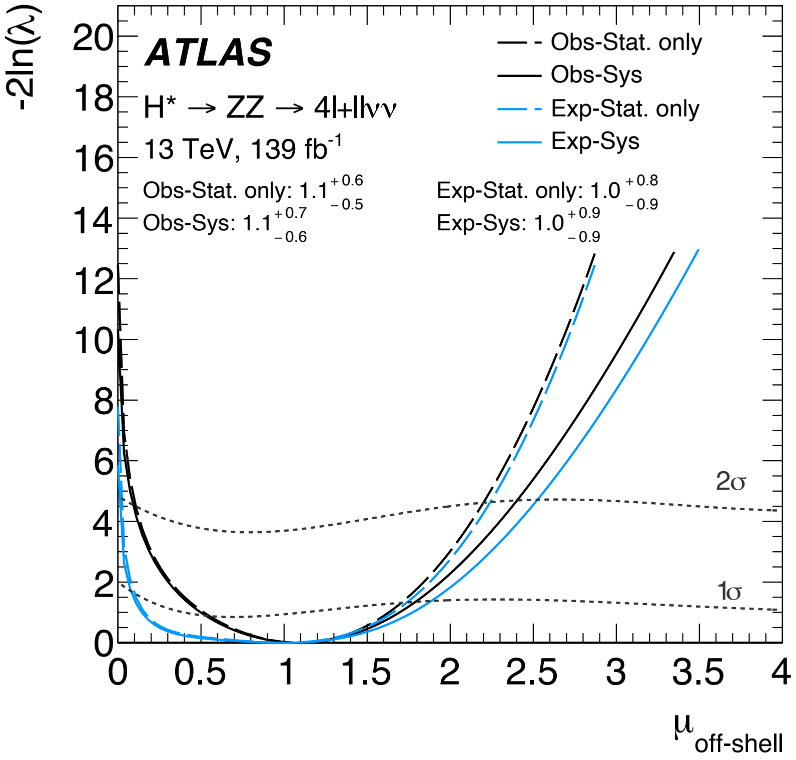

ATLAS Run 2 Γ_H measurement

The likelihood profile as a function of two off-shell signal strength parameters for the ggF and EW production modes

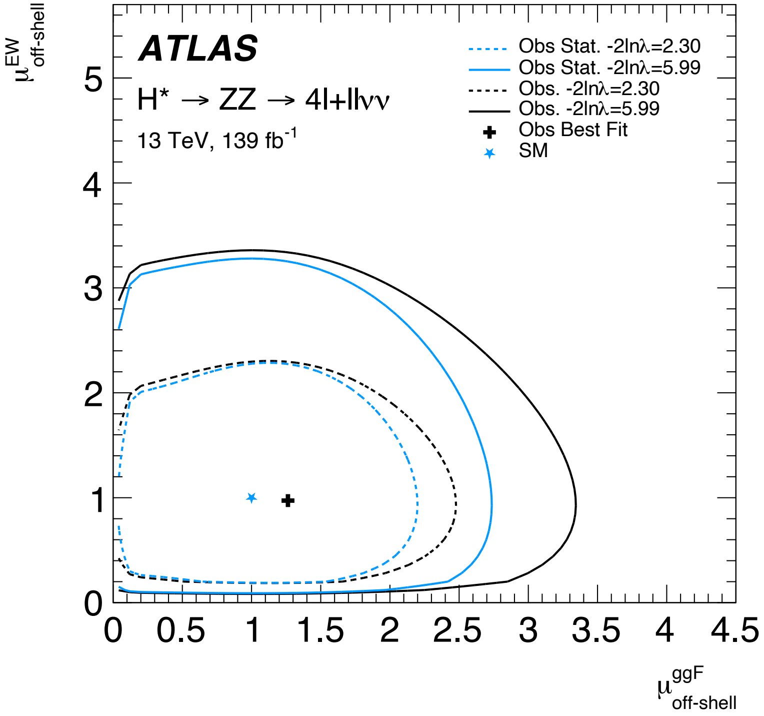

The likelihood profile as a function of the ratio of on-shell and off-shell coupling modifiers

$$R_{gg} = \frac{\kappa^2_{g,off-shell}}{\kappa^2_{g,on-shell}} \qquad R_{VV} = \frac{\kappa^2_{V,off-shell}}{\kappa^2_{V,on-shell}}$$

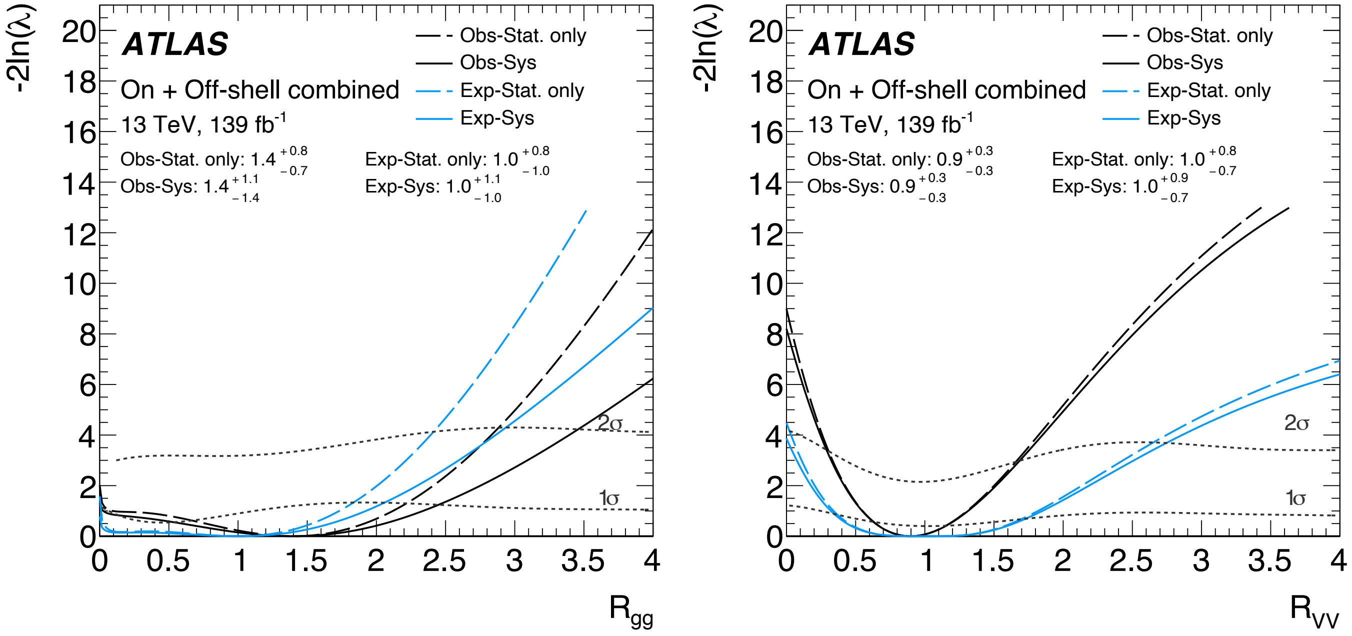

ATLAS Run 2 Γ_H measurement

Systematic uncertainties

Systematic Uncertainty Fixed	$\mu_{\text{off-shell}}$ value at which $-2\ln\lambda(\mu_{\text{off-shell}}) = 4$
Parton shower uncertainty for $gg \to ZZ$ (normalisation)	2.26
Parton shower uncertainty for $gg \to ZZ$ (shape)	2.29
NLO EW uncertainty for $qq \to ZZ$	2.27
NLO QCD uncertainty for $gg \to ZZ$	2.29
Parton shower uncertainty for $qq \to ZZ$ (shape)	2.29
Jet energy scale and resolution uncertainty	2.26
None	2.30

Phys. Lett. B 846 (2023) 138223

- Constraints are **statistically limited**
- Leading uncertainties from **theoretical modelling**, mainly **missing higher order for background** and **Parton shower**

Higgs production and decay modes

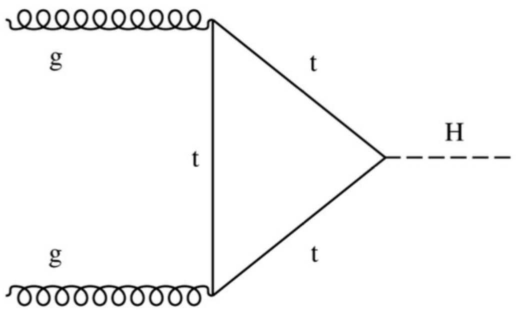

ggF, σ_{ggF}~48.5 pb

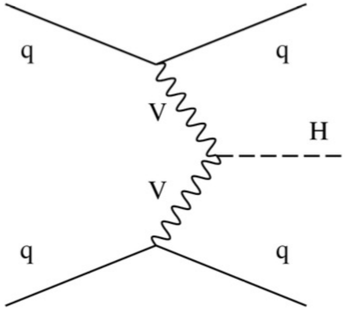

VBF, σ_{VBF}~3.8 pb

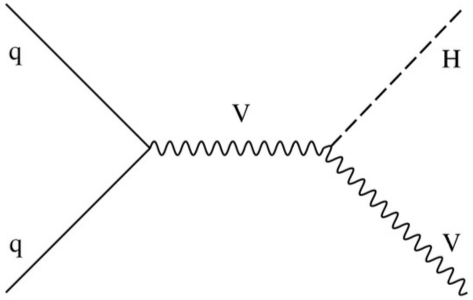

VH = WH or ZH, σ_{WH}~1.4 pb

σ_{ZH}~0.88 pb

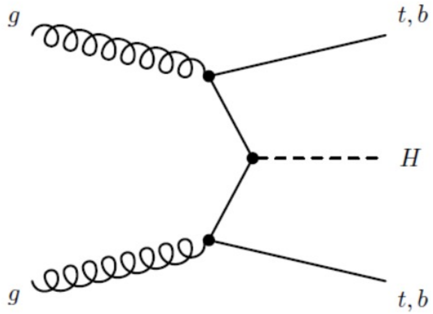

$t\bar{t}$H and $b\bar{b}$H, σ_{ttH}~0.51 pb

σ_{bbH}~0.49 pb

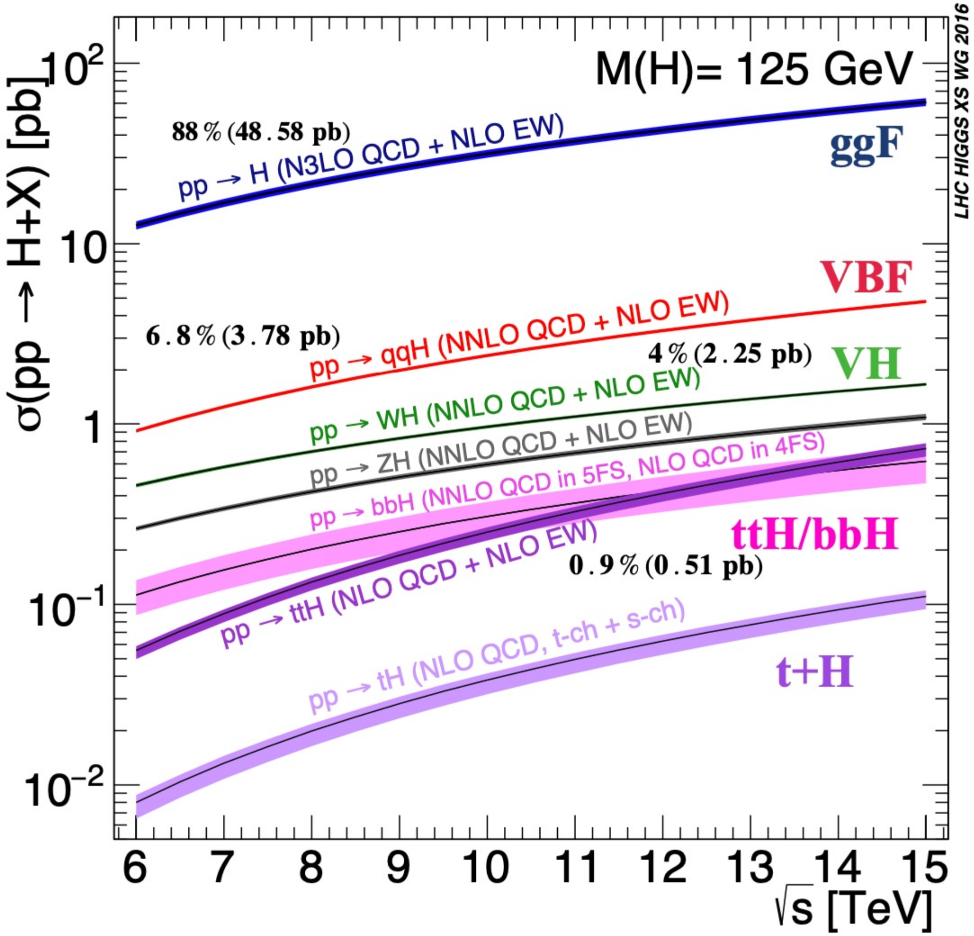

Higgs production and decay modes

- H → $b\bar{b}$: BR ~ 58.1 %
- H → WW*(→lνlν): BR ~ 21.5 %
- …
- H → ZZ*: BR ~ 2.6 %
  ZZ*→ 4l: BR ~ 0.0125%
- H → γγ: BR ~ 0.227%